REFERENCES

1 Yoshizawa H. Hepatocellular carcinoma associated with hepatitis C virus infection in Japan: projection to other countries in the foreseeable future. *Oncology* 2002; 62(Suppl. 1): 8–17.

2 Tsukuma H, Tanaka H, Ajiki W, Oshima A. Liver cancer and its prevention. *Asian Pac J Cancer Prev* 2005; 6: 44–50.

3 Tanaka H, Tsukuma H. Characteristics of Japanese patients with liver cancer – epidemiological study based on a comparison between male and female patients. *Hepatol Res* 2002; 24: S11–S20.

4 Tanaka Y, Kurbanov F, Mano S *et al.* Molecular tracing of the global hepatitis C virus epidemic predicts regional patterns of hepatocellular carcinoma mortality. *Gastroenterology* 2006; 130: 703–714.

5 Tanaka H, Imai Y, Hiramatsu N *et al.* Declining incidence of hepatocellular carcinoma in Osaka, Japan, from 1990 to 2003. *Ann Intern Med* 2008; 148: 820–826.

6 Tanaka H, Hiyama T, Tsukuma H *et al.* Prevalence of second generation antibody to hepatitis C virus among voluntary blood donors in Osaka, Japan. *Cancer Causes Control* 1994; 5: 409–413.

7 Tanaka H, Tsukuma H, Kasahara A *et al.* Effect of interferon therapy on the incidence of hepatocellular carcinoma and mortality of patients with chronic hepatitis C: a retrospective cohort study of 738 patients. *Int J Cancer* 2000; 87: 741–749.

8 Yoshida H, Arakawa Y, Sata M *et al.* Interferon therapy prolonged life expectancy among chronic hepatitis C patients. *Gastroenterology* 2002; 123: 483–491.

9 Kasahara A, Tanaka H, Okanoue T *et al.* Interferon treatment improves survival in chronic hepatitis C patients showing biochemical as well as virological responses by preventing liver-related death. *J Viral Hepat* 2004; 11: 148–156.

10 Imai Y, Kasahara A, Tanaka H *et al.* Interferon therapy for aged patients with chronic hepatitis C: improved survival in patients exhibiting a biochemical response. *J Gastroenterol* 2004; 39: 1069–1077.

11 Mazzella G, Accogli E, Sottili S *et al.* Alpha interferon treatment may prevent hepatocellular carcinoma in HCV-related liver cirrhosis. *J Hepatol* 1996; 24: 141–147.

12 Fattovich G, Giustina G, Degos F *et al.* Effectiveness of interferon alfa on incidence of hepatocellular carcinoma and decompensation in cirrhosis type C European Concerted Action on Viral Hepatitis (EUROHEP). *J Hepatol* 1997; 27: 201–205.

13 Imai Y, Kawata S, Tamura S *et al.* Relationship of interferon therapy and hepatocellular carcinoma in patients with chronic heaptitis C. *Ann Intern Med* 1998; 129: 94–99.

14 Nishiguchi S, Kuroki T, Nakatani S *et al.* Randomised trial of effects if interferon-α on incidence of hepatocellular carcinoma in chronic active hepatitis C with cirrhosis. *Lancet* 1995; 346: 1051–1055.

15 Kasahara A, Hayashi N, Mochizuki K *et al.* Risk factors for hepatocellular carcinoma and its incidence after interferon treatment in patients with chronic hepatitis C. *Hepatology* 1998; 27: 1394–1402.

16 Yoshida H, Shiratori Y, Moriyama M *et al.* Interferon therapy reduces the risk for hepatocellular carcinoma: national surveillance program of cirrhotic and noncirrhotic patients with chronic hepatitis C in Japan. *Ann Intern Med* 1999; 131: 174–181.

17 Ikeda K, Saitoh S, Arase Y *et al.* Effect of interferon therapy on hepatocellular carcinogenesis in patients with chronic hepatitis type C: a long-term observation study of 1,643 patients using statistical bias correction with proportional hazard analysis. *Hepatology* 1999; 29: 1124–1130.

18 Kurokawa M, Hiramatsu N, Oze T *et al.* Effect of interferon alpha-2b plus ribavirin therapy on incidence of hepatocellular carcinoma in patients with chronic hepatitis. *Hepatol Res* 2009; 39: 432–438.

19 Manns MP, McHutchison JG, Gordon SC *et al.* Peginterferon alfa-2b plus ribavirin compared with interferon alfa-2b plus ribavirin for initial treatment of chronic hepatitis C: a randomised trial. *Lancet* 2001; 358: 958–965.

20 Fried MW, Shiffman ML, Reddy KR *et al.* Peginterferon alfa-2a plus ribavirin for chronic hepatitis C virus infection. *N Engl J Med* 2002; 347: 975–982.

21 Hoofnagle JH, Seeff LB. Peginterferon and ribavirin for chronic hepatitis C. *N Engl J Med* 2006; 355: 2444–2451.

22 Arase Y, Ikeda K, Suzuki F *et al.* Prolonged-interferon therapy reduces hepatocarcinogenesis in aged-patients with chronic hepatitis C. *J Med Virol* 2007; 79: 1095–1102.

23 Di Bisceglie AM, Shiffman ML, Everson GT *et al.* Prolonged therapy of advanced chronic hepatitis C with low-dose peginterferon. *N Engl J Med* 2008; 359: 2429–2441.

24 Lok AS, Seeff LB, Morgan TR *et al.* Incidence of hepatocellular carcinoma and associated risk factors in hepatitis C-related advanced liver disease. *Gastroenterology* 2009; 136: 138–148.

25 Kato N, Yokosuka O, Omata M, Hosoda K, Ohto M. Detection of hepatic C virus ribonucleic acid in the serum by amplification with polymers chain reaction. *J Clin Invest* 1990; 86: 1764–1767.

26 Murakami R, Tsukuma H, Ubukata T *et al.* Estimation of validity of mass screening program for gastric cancer in Osaka, Japan. *Cancer* 1990; 65: 1255–1260.

27 Desmet VJ, Gerber M, Hoofnagle JH, Manns M, Sheuer PJ. Classification of chronic hepatitis: grading and staging. *Hepatology* 1994; 19: 1513–1520.

28 Knodell RG, Ishak KG, Black WC *et al.* Formulation and application of numerical scoring system for assessing histological activity in asymptomatic chronic active hepatitis. *Hepatology* 1981; 1: 431–435.

29 Ikeda K, Saitoh S, Koida I *et al.* A multivariate analysis of risk factors for hepatocellular carcinogenesis: a prospective observation of 795 patients with viral and alcoholic cirrhosis. *Hepatology* 1993; 18: 47–53.

30 Moriya K, Fujie H, Shintani Y *et al.* The core protein of hepatitis C virus induces hepatocellular carcinoma in transgenic mice. *Nat Med* 1998; 4: 1065–1067.

31 Moriya K, Nakagawa K, Santa T *et al.* Oxidative stress in the absence of inflammation in a mouse model for hepatitis C virus-associated hepatocarcinogenesis. *Cancer Res* 2001; 61: 4365–4370.

32 Makiyama A, Itoh Y, Kasahara A *et al.* Characteristics of patients with chronic hepatitis C who develop hepatocellular carcinoma after sustained response to interferon therapy. *Cancer* 2004; 101: 1616–1622.

© 2009 Blackwell Publishing Ltd

J Gastroenterol (2010) 45:244–248
DOI 10.1007/s00535-009-0159-y

RAPID COMMUNICATION

STAT3 signaling within hepatocytes is required for anemia of inflammation in vivo

Ryotaro Sakamori · Tetsuo Takehara · Tomohide Tatsumi · Minoru Shigekawa · Hayato Hikita · Naoki Hiramatsu · Tatsuya Kanto · Norio Hayashi

Received: 26 August 2009 / Accepted: 26 October 2009 / Published online: 1 December 2009
© Springer 2009

Abstract
Background Anemia of inflammation, commonly observed in patients with chronic diseases, is associated with decreased serum iron. Hepcidin, mainly produced by hepatocytes in a STAT3- and/or SMAD-dependent manner, is involved in iron homeostasis. What remains to be established is whether or not the hepatic IL-6/STAT3 signal has a role in anemia of inflammation in vivo.
Methods Turpentine oil was subcutaneously injected into wild-type mice or hepatocyte-specific STAT3-deficient mice (L-STAT3KO) to induce inflammation.
Results Turpentine injection increased serum IL-6 levels. It activated liver STAT3 in wild-type mice, but not in L-STAT3KO mice. In chronic inflammation, wild-type mice showed decreased serum iron levels and anemia with up-regulation of hepcidin levels in the liver. In contrast, L-STAT3KO mice showed no increase in hepatic hepcidin levels or anemia.
Conclusions Liver STAT3 is critically involved in the development of anemia of inflammation via the expression of hepcidin. The liver regulates anemia of inflammation through STAT3 signaling.

R. Sakamori · T. Takehara · T. Tatsumi · M. Shigekawa · H. Hikita · N. Hiramatsu · T. Kanto · N. Hayashi (✉)
Department of Gastroenterology and Hepatology,
Osaka University Graduate School of Medicine,
2-2 Yamada-oka, Suita, Osaka 565-0871, Japan
e-mail: hayashin@gh.med.osaka-u.ac.jp

Keywords Hepcidin · Anemia · STAT3 · Liver · Iron

Introduction

Hepcidin, a peptide hormone produced by hepatocytes, mediates interactions between the immune system and iron metabolism. As the key regulator of transmembrane iron transport, hepcidin controls the absorption of iron in the intestine, the mobilization of iron from hepatic stores, and iron recycling by macrophages. Hepcidin production is up-regulated by excess body iron and inflammation [1, 2] and down-regulated by anemia [2].

During inflammation, IL-6 rapidly induces hepcidin synthesis and corresponding hypoferremia [3]. The discovery that hepcidin expression is directly regulated by inflammatory cytokines has linked hepcidin to anemia of inflammation [4, 5], which is commonly observed in patients with chronic diseases and is associated with decreased serum iron and iron-laden bone marrow macrophages [6]. Anemia of inflammation is characterized by increased uptake and retention of iron by cells of the reticuloendothelial system, leading to low serum iron levels despite adequate iron stores. Under inflammatory circumstances, hepatic STAT3 is the key transcription factor responsible for IL-6-induced activation of hepcidin gene expression [7]. The liver is a very important organ for hepcidin expression, but there has been no report of the liver regulating anemia of inflammation.

In the present study, we used hepatocyte-specific STAT3-deficient mice (L-STAT3 KO) and examined the significance of STAT3 signaling within hepatocytes in anemia of inflammation. We found in vivo evidence for the necessity of STAT3 for anemia of inflammation.

Materials and methods

Animals

Five-week-old BALB/cA female mice purchased from CLEA Japan, Inc. (Tokyo, Japan) were used for the experimental iron overload. Mice carrying a STAT3 gene with 2 *loxP* sequences flanking exon 22 and a STAT3 null allele (STAT3 fl/−) have been described previously [8]. To generate mice with hepatocyte-specific STAT3 deficiency, we crossed STAT3 fl/− mice and Alb-Cre transgenic mice [9], which express the Cre recombinase gene under regulation of the albumin gene promoter. We crossed Alb-Cre STAT3 fl/fl mice and STAT3 fl/−. The resulting Alb-Cre STAT3 fl/− mice and Alb-Cre STAT3 fl/fl mice were used as L-STAT3 KO mice. Gender-matched STAT3 fl/− mice and STAT3 fl/fl mice obtained from the same litter were used as control mice. Although the data are not shown, there was no difference in hepcidin expression between STAT3 fl/fl mice and STAT3 fl/− mice upon turpentine injection. All animals were housed under specific pathogen-free conditions and treated with humane care under approval from the Animal Care and Use Committee of Osaka University Medical School.

Inflammation

Chronic inflammation was produced by subcutaneous injection of turpentine oil (0.1 ml/20 g of body weight; Nacalai Tesque, Kyoto, Japan) into the intrascapular fat pad at weekly intervals for 2 weeks (three injections per week). Control mice were similarly injected with an equivalent volume of sterile saline solution.

Hematological analysis and measurement of serum cytokine of mice

Blood samples were obtained 72 h after chronic turpentine injection and collected in heparinized tubes. Blood cell counts and erythrocyte parameters were determined using an automatic blood analyzer. Iron levels were measured using Quickauto-Neo Fe (SHINO-TEST Corp., Kanagawa, Japan). The level of IL-6 in the serum was measured using commercially available enzyme-linked immunosorbent assay (ELISA) kits.

Real-time reverse-transcription PCR

cDNA, equivalent to 50 ng RNA, was used as a template for real-time reverse-transcription PCR (RT-PCR) using an Applied Biosystems 7900HT Fast Real-Time PCR System (Applied Biosystems, Foster City, CA). Hepcidin messenger RNA (mRNA) expression was measured using TaqMan Gene Expression Assays (Assay ID Mm00519025_m1) and was corrected with the quantified expression level of glyceraldehyde-3-phosphate dehydrogenase (G3PDH) mRNA measured using TaqManGene Expression Assays (Assay ID Mm99999915_g1). All samples were assayed in triplicate.

Western blot analysis

We isolated liver protein from L-STAT3 KO mice and control littermates and performed Western blot analysis as previously described [10].

Statistics

Data are expressed as mean ± SD and compared using the Mann–Whitney test. Statistical significance was set at $P < 0.05$.

Results

During the inflammatory process, hepcidin gene expression is dramatically induced, resulting in anemia with iron deficiency

Subcutaneous injection of turpentine is a classical and widely accepted model of inflammation in mice [2, 3]. This treatment induces a variety of inflammatory cytokines such as IL-6 and TNF alfa. Previous research has revealed a predominant role of IL-6 in pathogenesis during turpentine-induced inflammation [10]. When wild-type mice were intra-subcutaneously injected with turpentine, hepatic STAT3 was activated (Fig. 1a). Hepcidin mRNA expression in the liver was increased after a single turpentine injection to Balb/cA mice (Fig. 1b), which resulted in up-regulation of the hepcidin gene during inflammatory states. As shown in Fig. 1c, a repeated injection of turpentine for 2 weeks resulted in a decrease of serum iron and an increase of unsaturated iron-binding capacity (UIBC). This chronic treatment resulted in anemia with reduction of key blood parameters, i.e., red blood cell, hemoglobin, and hematocrit (Fig. 1d).

Anemia of inflammation does not occur in L-STAT3 KO mice

Next we treated L-STAT3 KO mice in the same way. Turpentine oil raised serum IL-6 in both L-STAT3 KO mice and control littermates without any significant difference, but with tendency was higher in L-STAT3 KO mice (Fig. 2a). Hepatic STAT3 was activated by turpentine injection in control mice but not in L-STAT3 KO mice

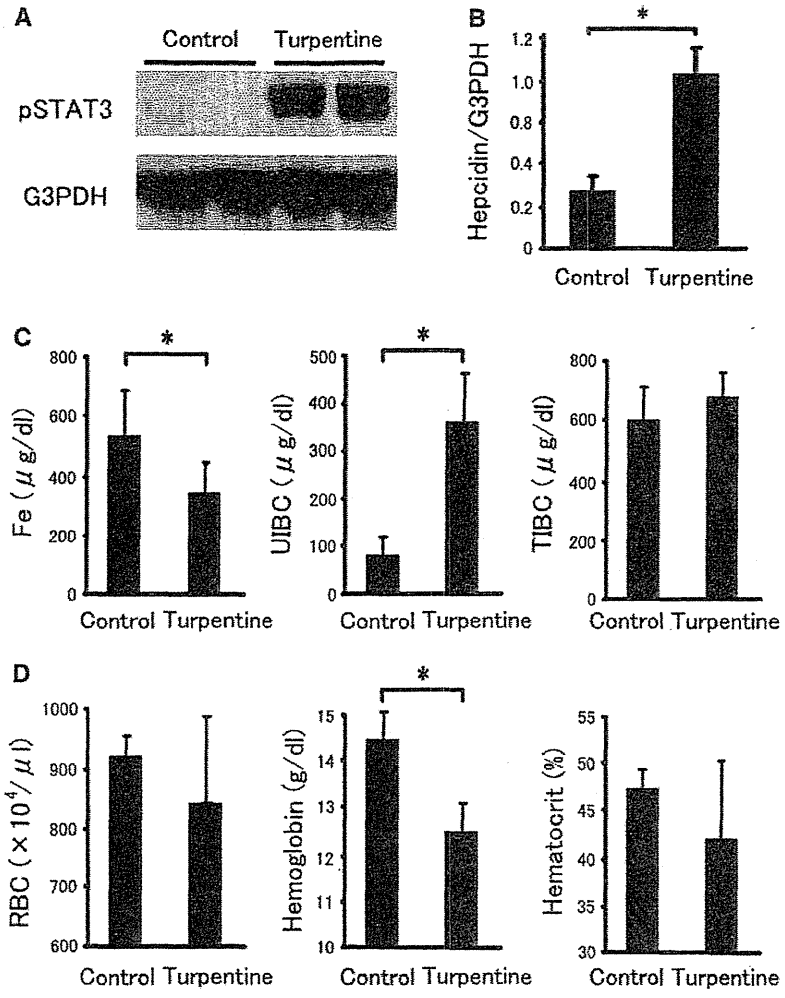

Fig. 1 Liver STAT3 activation, hepcidin mRNA expression, and hematological indices in turpentine-treated Balb/cA mice. **a** Liver lysates from mice after turpentine single injection (16 h) were analyzed by Western blot with an antibody to phosphorylation STAT3 and with an antibody to G3PDH as the loading control. **b** Relative changes in hepcidin mRNA level in the liver after single injection of turpentine (24 h); $n = 12$ for control mice and $n = 8$ for turpentine mice; $^*P < 0.05$. **c** Iron parameters in mice following chronic turpentine treatment; $n = 7$ for each group; $^*P < 0.05$. **d** Hematological parameters in mice following chronic turpentine treatment; $n = 4$ for control mice and $n = 6$ turpentine mice; $^*P < 0.05$

(Fig. 2b). Hepcidin mRNA expression in the liver was increased after turpentine injection, but was not observed in L-STAT3 KO mice (Fig. 2c). To check whether hepatocyte-STAT3 is required for anemia of inflammation, we measured the blood parameters of both mice. As shown in Fig. 2d, anemia after chronic treatment was observed in control mice, but not in L-STAT3 KO mice. Additionally, there was no significant difference in other blood parameters, i.e., white blood cells and platelets (Fig. 2e).

Discussion

In this research, we demonstrated that hepatic STAT3 regulates anemia of inflammation via hepcidin expression in vivo. Hepcidin expression can be up-regulated by high iron levels or during acute phase inflammatory responses. Each pathway of hepcidin expression has been reported in the BMP/SMAD pathway and the IL-6/STAT3 pathway. Hepcidin expression is thought to be due to the interaction between SMAD and STAT3 [12]. For example, the effect of IL-6 on hepcidin expression depends on SMAD4, as evidenced by the failure of IL-6 to increase hepcidin expression in mice with hepatocellular knockout of SMAD4 [12]. However, we found that hepatic STAT3 was not necessary for hepcidin expression through the SMAD pathway in the presence of iron excess (data not shown).

With respect to hepcidin expression, the BMP/SMAD pathway has been well studied [13]. Many reports state that the IL-6/STAT3 pathway regulates the expression of hepcidin in inflammation [7], but none comment on the IL-6/STAT3 pathway regulating anemia of inflammation. We therefore examined whether the liver could control anemia of inflammation via the IL-6/STAT3 pathway. In this experiment, we used L-STAT3 KO mice, which have the ability to intercept the inflammatory signals. Hepatic STAT3 is necessary for hepcidin expression during systemic inflammation, and thus the IL-6/STAT3 pathway in the liver can be expected to be involved with the immune system. It is well known that during chronic disease the

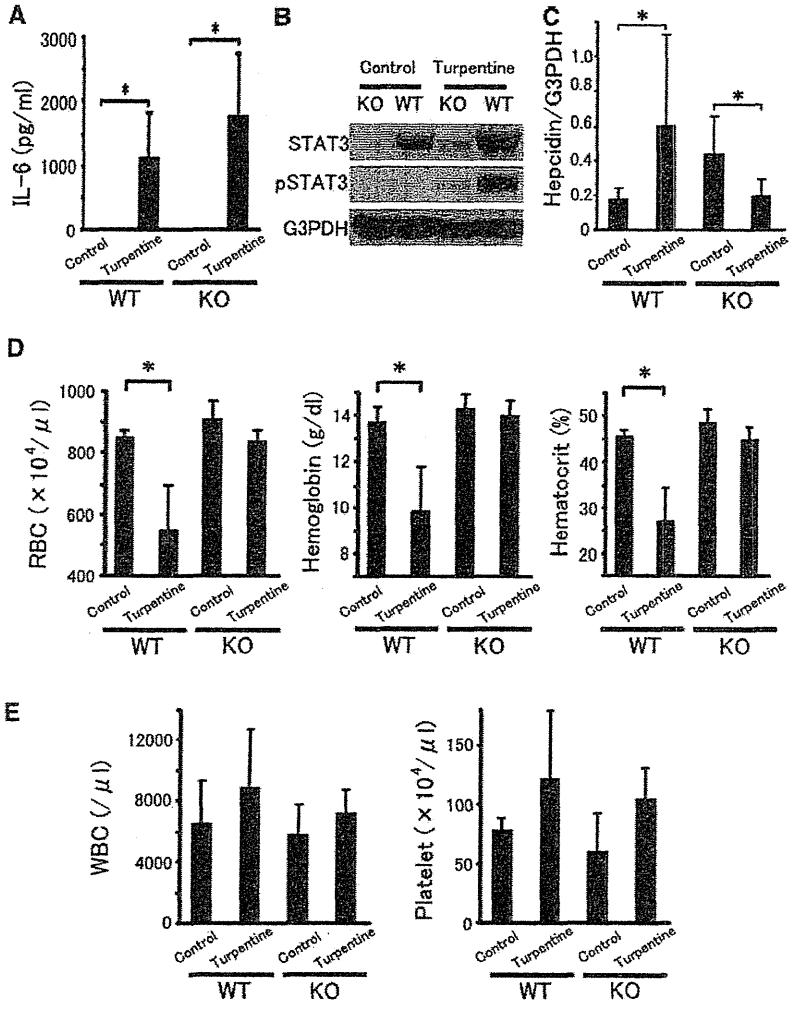

Fig. 2 Serum IL-6 levels, liver STAT3 activation, hepcidin mRNA expression, and hematological indices after turpentine injection in L-STAT3 KO mice and wild-type mice. **a** Serum IL-6 of L-STAT3 KO mice ($n = 10$) and control littermates ($n = 12$) after single injection of turpentine (24 h) or physiological saline; $n = 4$ for each group; $^*P < 0.05$. **b** Liver lysates from mice given a single injection of turpentine were analyzed by Western blot with an antibody to STAT3 and phosphorylation STAT3, and with an antibody to G3PDH as the loading control (24 h). **c** Relative changes in hepcidin mRNA level after chronic treatment in both L-STAT3 KO mice ($n = 10$) and control littermates ($n = 12$). As control group, L-STAT3 KO mice and control littermates were injected with physiological saline; $n = 4$ for each group; $^*P < 0.05$. **d** Red blood cells, hemoglobin and hematocrit in mice following chronic turpentine treatment in L-STAT3 KO mice ($n = 4$) and control littermates ($n = 6$). As control group, L-STAT3 KO mice and wild-type mice were injected with physiological saline; $n = 4$ for each group; $^*P < 0.05$. **e** White blood cells and platelets in mice following chronic turpentine treatment in L-STAT3 KO mice ($n = 4$) and control littermates ($n = 6$). As control group, L-STAT3 KO mice and wild-type mice were injected with physiological saline; $n = 4$ for each group

circulating levels of IL-6 are increased, resulting in an up-regulation of hepcidin activity and subsequent decreases in serum iron levels that may eventually lead to anemia [3]. Moreover, research has shown that STAT3 signaling within hepatocytes controls attenuation of the systemic inflammatory response and lethality during sepsis [11]. On the other hand, under the influence of elevated hepcidin concentrations, the macrophages, hepatocytes, and enterocytes retain iron that would otherwise be released into the plasma. This induced state of hypoferremia contributes to host immunity as invading microorganisms would find only a limited amount of plasma iron if the iron had been shifted from the circulation into cellular stores. For example, macrophages limit the intracellular growth of bacteria during iron depletion [14]. However, hypoferremia also limits the availability of iron for erythropoiesis, thereby contributing to the anemia associated with infection and inflammation [15]. The result of infection/inflammatory-mediated up-regulation in hepcidin levels is iron sequestration in macrophages and decreases in the absorption of

iron from the small intestine [4], eventually resulting in anemia. This is thought to be the relationship between the IL-6/STAT3 pathway in the liver and the host defense system that works against infecting microorganisms. In other words, liver STAT3 may control host immunity by causing anemia with iron deficiency. In summary, the present data indicate that anemia of inflammation is regulated by liver STAT3, which may be involved with the systemic immune system.

Acknowledgments We thank Dr. S. Akira and Dr. K. Takeda for providing STAT3 floxed mice. This work was supported by a Grant-in-Aid for Scientific Research from the Ministry of Education, Culture, Sports, Science, and Technology, Japan.

Conflict of interest statement No conflicts of interest exist.

References

1. Pigeon C, Ilyin G, Courselaud B, Leyroyer P, Turlin B, Brissot P, et al. A new mouse liver-specific gene, encoding a protein homologous to human antimicrobial peptide hepcidin, is overexpressed during iron overload. J Biol Chem. 2001;276:7811–9.
2. Nicholas G, Chauvet C, Viatte L, Danan JL, Bigard X, Devaux I, et al. The gene encoding the iron regulatory peptide hepcidin is regulated by anemia, hypoxia, and inflammation. J Clin Invest. 2002;110:1037–44.
3. Nemeth E, Rivera S, Gabayan V, Keller C, Taudorf S, Pedersen BK, et al. IL-6 mediates hypoferremia of inflammation by inducing the synthesis of the iron regulatory hormone hepcidin. J Clin Invest. 2004;113:1271–6.
4. Ganz T. Hepcidin, a key regulator of iron metabolism and mediator of anemia of inflammation. Blood. 2003;102:783–8.
5. Roy CN, Andrews NC. Anemia of inflammation: the hepcidin link. Curr Opin Hematol. 2005;12:107–11.
6. Weinstein DA, Roy CN, Fleming MD, Loda MF, Wolfsdorf JI, Andrews NC. Inappropriate expression of hepcidin is associated with iron refractory anemia: implications for the anemia of chronic disease. Blood. 2002;100:3776–81.
7. Pietrangelo A, Dierssen U, Valli L, Garuti C, Rump A, Corradini E, et al. STAT3 is required for IL-6-gp130-dependent activation of hepcidin in vivo. Gastroenterology. 2007;132:294–300.
8. Takeda K, Kaisho T, Yoshida N, Takeda J, Kishimoto T, Akira S. Stat3 activation is responsible for IL-6-induced T cell proliferation through preventing apoptosis: generation and characterization of T cell-specific Stat3-deficient mice. J Immunol. 1998;161:4652–60.
9. Takehara T, Tatsumi T, Suzuki T, Rucker EB 3rd, Hennighausen L, Jinushi M, et al. Hepatocyte-specific disruption of Bcl-xL leads to continuous hepatocyte apoptosis and liver fibrotic responses. Gastroenterology. 2004;127:1189–97.
10. Geller DA, Kispert PH, Su GL, Wang SC, Di Silvio M, Tweardy DJ, et al. Induction of hepatocyte lipopolysaccharide binding protein in models of sepsis and the acute-phase response. Arch Surg. 1993;128:22–7.
11. Sakamori R, Takehara T, Ohnishi C, Tatsumi T, Ohkawa K, Takeda K, et al. Signal transducer and activator of transcription 3 signaling within hepatocytes attenuates systemic inflammatory response and lethality in septic mice. Hepatology. 2007;46:1564–73.
12. Wang RH, Li C, Xu X, Zheng Y, Xiao C, Zerfas P, et al. A role of SMAD4 in iron metabolism through the positive regulation of hepcidin expression. Cell Metab. 2005;2:399–409.
13. Babitt JL, Huang FW, Wrighting DM, Xia Y, Sidis Y, Samad TA, et al. Bone morphogenetic protein signaling by hemojuvelin regulates hepcidin expression. Nat Genet. 2006;38:531–9.
14. Paradkar PN, De Domenico I, Durchfort N, Zonh I, Kaplan J, Ward DM. Iron depletion limits intracellular bacterial growth in macrophage. Blood. 2008;112:866–74.
15. Andrews NC. Anemia of inflammation: the cytokine–hepcidin link. J Clin Invest. 2004;113:1251–3.

Cancer Immunol Immunother (2010) 59:759–767
DOI 10.1007/s00262-009-0796-2

ORIGINAL ARTICLE

EphA2-derived peptide vaccine with amphiphilic poly(γ-glutamic acid) nanoparticles elicits an anti-tumor effect against mouse liver tumor

Shinjiro Yamaguchi · Tomohide Tatsumi · Tetsuo Takehara · Akira Sasakawa · Masashi Yamamoto · Keisuke Kohga · Takuya Miyagi · Tatsuya Kanto · Naoki Hiramastu · Takami Akagi · Mitsuru Akashi · Norio Hayashi

Received: 21 August 2009 / Accepted: 10 November 2009 / Published online: 27 November 2009
© Springer-Verlag 2009

Abstract The prognosis of liver cancer remains poor, but recent advances in nanotechnology offer promising possibilities for cancer treatment. Novel adjuvant, amphiphilic nanoparticles (NPs) composed of L-phenylalanine (Phe)-conjugated poly(γ-glutamic acid) (γ-PGA-Phe NPs) having excellent capacity for carrying peptides, were found to have the potential for use as a peptide vaccine against tumor models overexpressing artificial antigens, such as ovalbumin (OVA). However, the anti-tumor potential of γ-PGA-Phe NPs vaccines using much less immunogenic tumor-associated antigen (TAA)-derived peptide needs to be clarified. In this study, we evaluated the effectiveness of immunization with EphA2, recently identified TAA, derived peptide-immobilized γ-PGA-Phe NPs (Eph-NPs) against mouse liver tumor of MC38 cells (EphA2-positive colon cancer cells). Immunization of normal mice with Eph-NPs resulted in generation of EphA2-specific type-1 CD8+ T cells. Immunization with Eph-NPs tended to provide a degree of anti-MC38 liver tumor protection more than that observed for immunization with the mixture of EphA2-derived peptide and complete Freund's adjuvant (Eph + CFA). Neither Eph-NPs nor Eph + CFA vaccines inhibited tumor growth of BL6, EphA2-negative melanoma cells. Splenocytes isolated from MC38-bearing mice treated with Eph-NPs showed strong and specific cytotoxic activity against MC38 cells. Immunization with Eph + CFA induced liver damage as evidenced by elevation of serum alanine aminotransferase, while Eph-NPs vaccination did not exhibit any toxic damage to the liver. These results demonstrated that immunization with Eph-NPs displayed anti-tumor effects against liver tumor by generating acquired immunity equivalent to the toxic adjuvant CFA, suggesting that safe γ-PGA-Phe NPs could be applied clinically for the vaccine treatment of liver cancer.

Keywords Peptide vaccine · EphA2-derived peptide · Acquired immunity · Liver tumor

Abbreviations

IFA	Incomplete Freund's adjuvant
NPs	Nanoparticles
γ-PGA	Poly(γ-glutamic acid)
Phe	L-Phenylalanine
CFA	Complete Freund's adjuvant
PBS	Phosphate buffered saline
i.p.	Intraperitoneal
ALT	Alanine aminotransferase
DCs	Dendritic cells

Introduction

Immunotherapies using peptide vaccine combined with immunologic adjuvants, such as incomplete Freund's

S. Yamaguchi and T. Tatsumi contributed equally to this work.

S. Yamaguchi · T. Tatsumi (✉) · T. Takehara · A. Sasakawa · M. Yamamoto · K. Kohga · T. Miyagi · T. Kanto · N. Hiramastu · N. Hayashi
Department of Gastroenterology and Hepatology, Osaka University Graduate School of Medicine, 2-2 Yamadaoka, Suita, Osaka 565-0871, Japan
e-mail: tatsumit@gh.med.osaka-u.ac.jp

T. Akagi · M. Akashi
Department of Applied Chemistry, Graduate School of Engineering, Osaka University, Suita, Japan

S. Yamaguchi · T. Tatsumi · T. Takehara · A. Sasakawa · M. Yamamoto · T. Akagi · M. Akashi · N. Hayashi
Core Research for Evolutional Science and Technology (CREST), Japan Science and Technology Agency (JST), Tokyo, Japan

adjuvant (IFA), saponin QS-21, and several cytokines, could enhance the anti-tumor immune response after immunization [1, 2]. To date, these therapies have been clinically applied to patients with several types of cancer and have shown limited anti-tumor effects [3–7]. This is because dose-limiting toxicities of the adjuvant were often observed or the adjuvant effects of the peptide vaccine were too weak to induce a sufficient anti-tumor effect. At present, only aluminum salt has been approved as an immunological adjuvant for clinical use; it appears to have weak activity as an adjuvant [8]. Thus, a new strategy using strong and safe immunologic adjuvant is needed to improve their clinical efficacy in cancer treatment. Recently, advances in nanotechnology have offered promise for application in medical science. Some investigators have reported testing various kinds of nanoparticles (NPs) using efficient antigen-carriers for their biological potential [9–11]. We previously demonstrated the efficacy of immunotherapies using HIV-capturing non-biodegradable polystyrene NPs in an animal model [12–15]. However, non-biodegradable polystyrene NPs would not be applicable in clinical situations as vaccine material due to their safety issues. To improve NP-based vaccines, we have successfully generated biodegradable NPs composed of poly(γ-glutamic acid) (γ-PGA) and hydrophobic amino acid, L-phenylalanine (Phe) [16]. γ-PGA is a naturally occurring poly(amino acid) that is synthesized by certain strains of *Bacillus*. The polymer is made of D- and L-glutamic acid units linked through the α-amino and the γ-carboxylic acid groups, respectively. γ-PGA is water soluble, biodegradable and edible. Therefore, the potential applications of γ-PGA and its derivatives have been of interest in a broad range of fields, including the medical field [17–19]. γ-PGA-Phe NPs can be degraded by γ-glutamyl transpeptidase [20], which is widely distributed in the entire body, and various molecules such as proteins and peptides can be immobilized on the surface or encapsulated into γ-PGA-Phe NPs [21]. We demonstrated that γ-PGA-Phe NPs have an excellent capacity for carrying various proteins and peptides into antigen-presenting cells such as dendritic cells (DCs) and macrophages [22]. However, previous reports were studies that examined the potential of vaccines with γ-PGA-Phe NPs using artificial antigens, such as OVA, which are much more immunogenic than tumor-associated self-antigens. The anti-tumor potential of tumor-associated antigen (TAA)-derived peptide vaccine must be examined in order to establish peptide vaccine therapy using γ-PGA-Phe NPs.

The liver is the most common site of distal metastasis for tumors developing in distal organs, such as the colon, stomach and pancreas, and the physiological status of this organ correlates with the survival of patients with advanced disease, even if the primary tumor site has been resected curatively [23, 24]. We demonstrated that the recently identified TAA EphA2 is overexpressed in colon cancer tissues and that EphA2-derived peptide pulsed DCs showed the high potential as a cancer vaccine in a mouse tumor model [25, 26], suggesting that EphA2-derived peptide could be applicable to evaluate the potential of peptide vaccines with γ-PGA-Phe NPs.

In the present study, we demonstrated that immunization with EphA2-derived peptide-immobilized γ-PGA-Phe nanoparticles (Eph-NPs) displayed anti-tumor effects against EphA2-expressing liver tumor by eliciting EphA2 antigen-specific acquired immunity equivalent to peptide vaccine using the strongest but very toxic adjuvant, complete Freund's adjuvant (CFA). These results indicate that peptide vaccine using γ-PGA-Phe NPs could be a promising candidate for a vaccine adjuvant against liver cancer.

Materials and methods

Mice

Female C57BL/6 mice were purchased from Clea Japan Inc. (Tokyo, Japan) and were used at 6–8 weeks of age. They were housed under conditions of controlled temperature and light with free access to food and water at the Institute of Experimental Animal Science, Osaka University Graduate School of Medicine. All animals received humane care and our study protocol complied with the institution's guidelines.

Cell lines

MC38 as EphA2-positive cell, a mouse colon carcinoma cell derived from C57BL6/J mice, was generously provided by Dr. Kazumasa Hiroishi (Showa University School of Medicine, Tokyo) [25]. BL6 as EphA2 negative cell, a melanoma cell line, and YAC-1, a sensitive cell line to NK cells were purchased from American Type Culture Collection (Rockville, MD) [25]. These cell lines were maintained in Complete Medium (RPMI medium supplemented with 10% fetal bovine serum, 100 U/ml penicillin and 100 μg/ml streptomycin) at 37°C in 5% CO_2.

Preparation of peptide-immobilized γ-PGA-Phe NPs

Nanoparticles composed of γ-PGA-Phe were prepared as previously described [27]. To prepare EphA2-derived peptide-immobilized NPs (Eph-NPs), a carboxyl group of the γ-PGA-Phe NPs (10 mg/ml) was first activated by water-soluble carbodiimide (1 mg/ml in 20 mM phosphate buffer, pH 5.8) for 20 min. The NPs (5 mg) obtained by centrifugation were mixed with 1 ml EphA2-derived peptide (0.5 mg/ml) in phosphate buffered saline (PBS)

and the mixture was incubated at 4°C for 24 h. After the reaction, the centrifuged NPs were washed three times with PBS and resuspended at 10 mg/ml in PBS. Eph-NPs immobilizing 20 μg of EphA2-derived peptide per 1 mg of NPs were prepared. The particle size distribution and the surface charge of NPs were measured by a dynamic light scattering (DLS) and zeta potential measurement using a Zetasizer Nano ZS (Malvern Instruments, UK). The mean diameters of NPs and Eph-NPs were 219 ± 78 and 246 ± 88 nm (mean ± SD), respectively. The NPs and Eph-NPs had a strongly negative zeta potential (−20 to −25 mV) in PBS.

IFN-γ ELISPOT assays for peptide-reactive CD8+ T cells responses

Splenocytes were harvested 5 days after intraperitoneal (i.p.) immunization of normal mice with various amounts of Eph-NPs or equal amounts of EphA2-derived peptide alone twice with a 1-week interval. In another experiments, splenocytes were harvested 5 days after i.p. immunization of normal mice with 10 μg of Eph-NPs or a mixture of 10 μg of EphA2-derived peptide with CFA (Eph + CFA), 10 μg of Eph peptide only (Eph), the γ-PGA-Phe NPs only (NPs) or PBS twice with a 1-week interval. CD8+ T cells were selectively isolated from splenocytes by magnetic cell sorting using CD8 MicroBeads (Miltenyi Biotec, Gladbach, Germany). Mouse IFN-γ ELISPOT assays were performed using a mouse IFN-γ ELISPOT kit (R&D Systems Inc., Minneapolis, MN) according to the manufacturer's instructions. IFN-γ-secreting cells appeared as blue spots. The data are represented as mean IFN-γ spots ± standard deviation (SD) per 100,000 CD8+ T cells analyzed.

Animal experiments

C57BL/6 mice were immunized intraperioneally with Eph-NPs, Eph + CFA, Eph, NPs or PBS twice a week as above. On day 0, at the time of the second injection with these vaccines, mice were lightly anesthetized by isoflurane and 1×10^6 MC38 cells (EphA2-positive) or 1×10^6 BL6 cells (EphA2-negative) were injected under the capsule of the left medial liver lobe by using a 30-gauge needle as previously described [26]. To prevent leakage, a cotton swab was held over the injection site for 2 min. Skin and peritoneum were closed in a single layer using a nylon suture. The procedure was well tolerated by all animals and no intraoperative or anesthesia-related deaths occurred. Mice were killed 14 days after tumor inoculation and the liver weight was measured. Data are reported as the average liver weights ± SD. All the protocols of animal experiments were approved by Institutional Animal Care and Use Committees of Osaka University Graduate School of Medicine.

Cytolytic assays

Splenocytes were harvested 14 days after tumor inoculation. After 5 days of in vitro stimulation with mitomycin C(MMC) (Kyowa Hakko, Tokyo, Japan)-treated MC38 cells, lymphocytes were analyzed for their ability to kill MC38 tumor cells in 4-h ^{51}Cr release assays as previously described [28]. In some experiments, liver lymphocytes were isolated 1 day after immunization of Eph-NPs into MC38-bearing mice as previously described [26], and subjected to 4-hr ^{51}Cr release assays against NK-sensitive YAC-1 target cells.

In vivo depletion of immune cells

The procedure used in this study was described previously [25]. The efficiency of specific subset depletions (CD4+, CD8+ T cell or NK cell) was confirmed by flow cytometric analysis. In all cases, 99% of the targeted cell subset was specifically depleted (data not shown).

Blood biochemistry test

Blood samples were obtained 7 days after final immunization. Levels of serum alanine aminotransferase (ALT), total bilirubin (TBil), albumin (Alb), and creatinine (Crnn) were measured with a standard UV method using a Hitachi type 7170 automatic analyzer (Tokyo, Japan).

Statistical analyses

Statistical differences between the groups were determined by applying Student's *t* test with Welch correction or one-way ANOVA after each group had been tested with equal variance and Fisher's exact probability tests. Statistical significance was defined as $P < 0.05$.

Results

Detection of EphA2-derived peptide-specific CD8+ T cells after immunization with Eph-NPs into normal mice

We performed IFN-γ ELISPOT assays to examine whether i.p. injection of Eph-NPs into normal mice could generate CD8+ T cells specific for EphA2-derived peptide. As shown in Fig. 1a, the frequencies of EphA2-derived peptide-specific CD8+ T cells in mice treated with the NPs immobilized with 10 or 50 μg of EphA2-derived peptides were significantly higher than those observed for mice

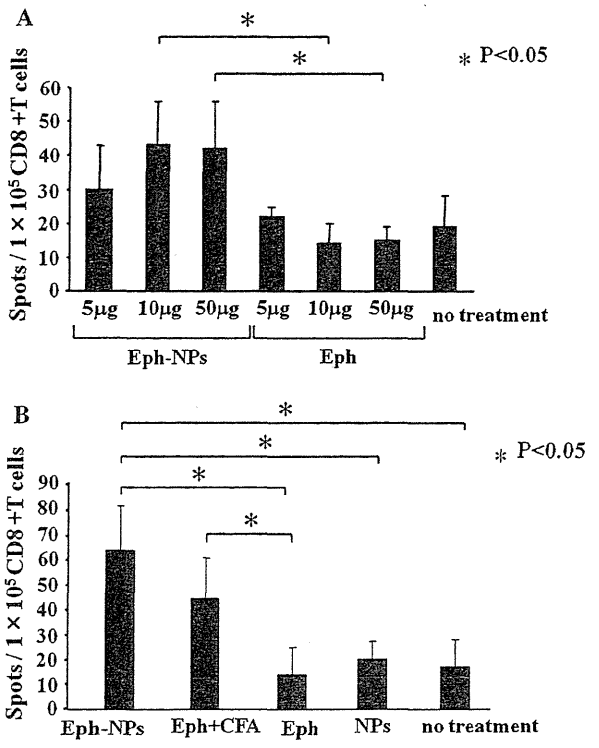

Fig. 1 IFN-γ ELISPOT assays for peptide-reactive CD8+ T cells responses. Normal mice ($N = 3$) were immunized with the indicated dose of Eph-NPs, Eph + CFA, Eph peptide only (*Eph*) or NPs only (*NPs*), and killed on day 5 post-immunization. Spleen cells were harvested and CD8+ T cells isolated using CD8 MicroBeads as described in "Materials and methods". CD8+ T cells were then subjected to IFN-γ ELISPOT assays to detect EphA2-derived peptide-specific CTLs. The data are represented as mean IFN-γ spots ± SD per 100,000 CD8+ T cells analyzed. Similar results were obtained in three independent experiments. $^*P < 0.05$

treated with equal amounts of peptides alone. The frequency of EphA2-derived peptide-specific cytotoxic T lymphocytes (CTLs) from mice immunized with the NPs immobilized with 10 μg of EphA2-derived peptides was equal to that from mice treated with NPs immobilized with 50 μg of EphA2-derived peptides. Thus, we used NPs immobilized with 10 μg of EphA2-derived peptides as Eph-NPs vaccines in the following experiments. As shown in Fig. 1b, the frequency of EphA2-derived peptide-specific CD8+ T cells in mice treated with the NPs immobilized with 10 μg of EphA2-derived peptides (Eph-NPs) was significantly higher than that observed for mice treated with NPs alone or EphA2-derived peptides alone. The frequency of EphA2-derived peptide-specific CTLs from mice immunized with Eph-NPs was equal to that from mice treated with mixture of 10 μg of EphA2-derived peptide with CFA (Eph + CFA). These results demonstrated that EphA2-specific type-1 CD8+ T cells (i.e. Tc1) are effectively generated by in vivo immunization with Eph-NPs.

Immunization with Eph-NPs prevents progression of EphA2-expressing liver tumors

We examined whether immunization with the Eph-NPs would promote protective anti-tumor effects against the EphA2-positive MC38 or EphA2-negative BL6 liver tumors. C57BL/6 mice were immunized on day −7 and 0 with Eph-NPs, Eph + CFA, EphA2-derived peptide only (Eph), NPs only (NPs) or PBS. On day 0, at the time of the second injection with these vaccines, mice were lightly anesthetized by isoflurane and 1×10^6 MC38 cells or 1×10^6 BL6 cells were injected under the capsule of the left medial liver lobe. Mice were killed 14 days after tumor inoculation and the liver weight was measured. As shown in Fig. 2a, the liver tumor from mice treated by Eph-NPs tended to be smaller than those from mice treated by Eph + CFA, Eph, NPs or PBS. The liver weights bearing MC38 tumor in mice immunized with Eph-NPs were significantly lighter than those in mice treated with Eph, NPs or PBS. In contrast, those in mice treated with Eph + CFA were not significantly lighter than those in control mice. The liver weights bearing MC38 tumor in mice treated with Eph-NPs tended to be lighter, but not significantly, than those with Eph + CFA (Fig. 2a). Neither Eph-NPs nor Eph + CFA inhibited BL6, EphA2 negative melanoma, tumor growth (Fig. 2b). These results suggest that immunization with Eph-NPs provides specific anti-tumor effects against EphA2-positive MC38 tumors. We also examined the liver weights of mice treated with Eph-NP, Eph + CFA, Eph, NPs or PBS without tumor injection. Mice were treated twice a week with each treatment without tumor injection and evaluated the liver weights 14 days after treatment. The liver weights from all treated mice without tumor injection were almost similar (data not shown), suggesting that each treatment did not affect the liver weight.

Induction of specific CTLs against MC38 cells after immunization with Eph-NPs into MC38 bearing mice

We examined whether immunization of Eph-NPs would induce tumor-specific cytolytic activity against MC38. As shown in Fig. 3a, splenocytes isolated from mice treated with Eph-NPs or Eph + CFA displayed stronger cytolytic activity against MC38 cells when compared with those immunized with EphA2-derived peptide alone, NP alone or PBS. Furthermore, splenocytes harvested from mice treated with Eph-NPs displayed a degree of anti-MC38 cytolytic activity equivalent to those immunized with Eph + CFA. On the other hand, the cytolytic activity was not observed against EphA2-negative BL6 cells in all treatment groups. We next examined whether lymphocytes isolated from the liver 1 day after tumor inoculation displayed cytolytic activity against a NK-sensitive cell, YAC-1 in vitro.

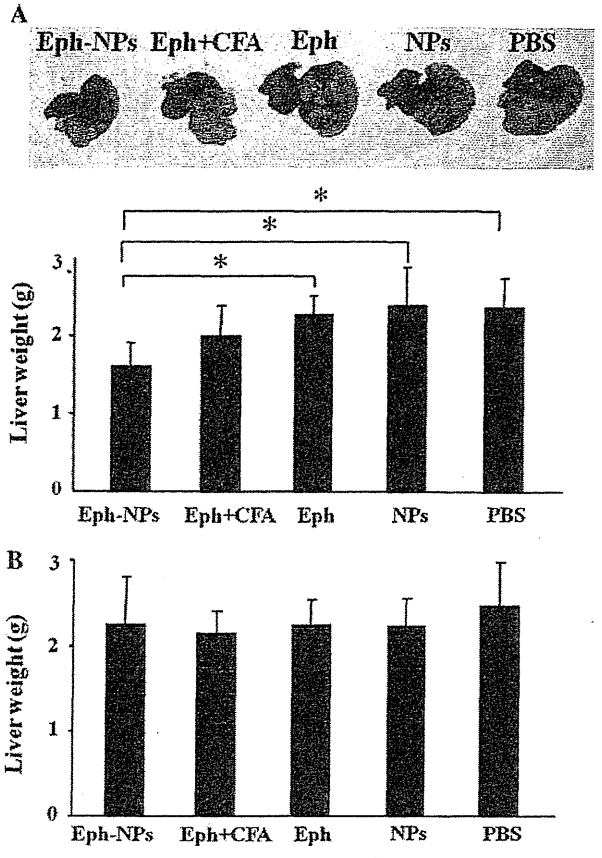

Fig. 2 Anti-tumor effects of immunization with Eph-NPs against liver tumor. C57BL/6 mice were immunized on day −7 and 0 with Eph-NPs, Eph + CFA, EphA2-derived peptide only (*Eph*), NPs only (*NPs*) or PBS. On day 0, 1×10^6 MC38 cells (**a**) or 1×10^6 BL6 cells (**b**) were injected intrahepatically. Fourteen days after immunization, mice were killed and liver weight was examined (**a** *upper panel*). Representative liver macroscopic view of each treatment group (**a** lower panel, **b**). Comparison of liver weight of each group. $*P < 0.05$. $N = 8$/group. Each data point represents the mean liver weight ± SD

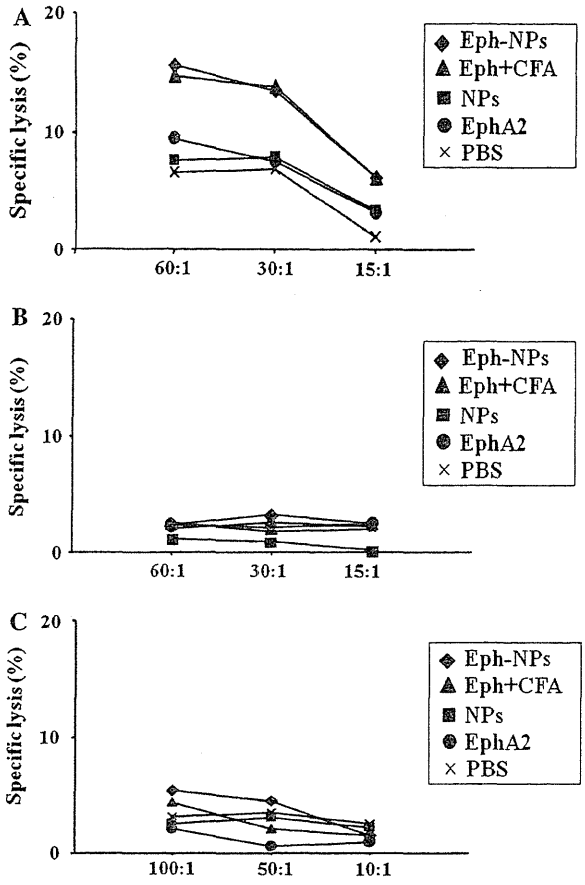

Fig. 3 Eph-NPs vaccines generated tumor-specific CTLs. Splenocytes were harvested from MC38 tumor-bearing mice 14 days after final treatment with Eph-NPs, Eph + CFA, NPs, Eph or PBS. Splenocytes were stimulated in vitro with MMC-treated MC38 cells for 5 days. The cytolytic activity of spleen cells was evaluated using 4-h ^{51}Cr release assays against MC38 (**a**) or irrelevant BL6 (**b**) tumor target cells at the indicated E:T ratios. **c** Liver lymphocytes were harvested 1 day after immunization into MC38-bearing mice. Liver lymphocytes were subjected to 4-h ^{51}Cr release assays against the NK-sensitive cells, YAC-1 as target cells at the indicated E:T ratios. Similar results were obtained in three independent experiments

No cytolytic activity was observed against a YAC-1 target cell in any of the control/treatment protocols (Fig. 3c). These results suggest that immunization using Eph-NPs or Eph + CFA effectively generated MC38-specific CTLs in vivo, which played essential roles in the liver tumor rejection.

Depletion of CD8+ T cells impairs the anti-tumor effects of immunization with Eph-NPs

To prove whether the therapeutic benefit associated with Eph-NPs vaccine in the MC38 liver tumor was dependent on CD4+, CD8+ T cells or NK cells, we performed selective cell subset depletion studies and C57BL/6 mice were immunized intraperioneally with Eph-NPs or PBS twice a week. On day 0, at the time of the second injection with these vaccines, mice were lightly anesthetized by isoflurane and 1×10^6 MC38 cells (EphA2-positive) were injected under the capsule of the left medial liver lobe as above. Mice were killed 14 days after tumor inoculation and the liver weight was measured. The anti-tumor efficacy of Eph-NPs immunization tended to be reduced in CD8+ T cell-depleted mice, while the liver weights of CD4+ T cell or NK cell-depleted mice were similar to those of non-depleted mice if the animals received Eph-NPs vaccines (Fig. 4). These results suggest that CD8+ T cells, but not CD4+ T cells or NK cells, tended to be required for optimal anti-tumor effects associated with Eph-NPs vaccines against liver tumor.

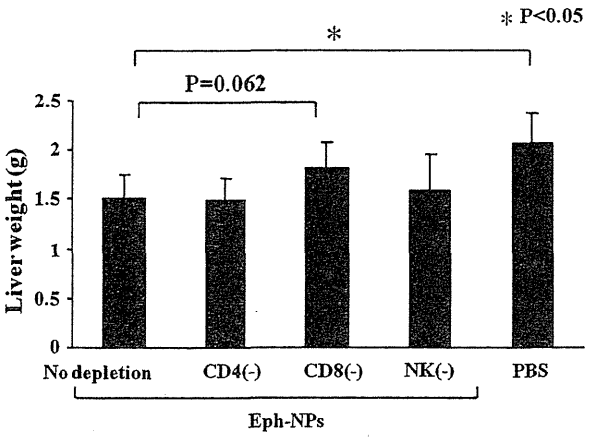

Fig. 4 Eph-NPs immunization tended to require CD8+ T cells, but not CD4+ T cells and NK cells in preventing liver tumor. Ab-mediated in vivo depletion of CD4+, CD8+ T cells, NK cells were performed (as described in "Materials and methods"), with the depleted mice then receiving Eph-NPs intraperitoneally (on day −7, 0) and 1×10^6 MC38 cells intrahepatically (day 0). Mice were killed 14 days after tumor inoculation and the liver weight was measured. $^*P < 0.05$. $N = 8$/group. Each data point represents the mean liver weight ± SD

Safety of Eph-NPs versus Eph + CFA

To evaluate the safety of Eph-NPs vaccine, the serum ALT, TBil, Alb and Crnn were examined for mice immunized with Eph-NPs, Eph + CFA, Eph, NPs or PBS as above. Immunization with Eph + CFA induced liver damage as evidenced by elevated serum ALT levels compared with those for mice treated with PBS. In contrast, other treatments did not lead to liver damage. There was no toxic effect on TBil, Alb and Crnn in all treatment groups (Fig. 5). Immunization with CFA induced granulomatous peritonitis in all of the mice, but immunization with the other regimens did not. These results demonstrated that the Eph + CFA vaccine is toxic to hepatocytes but the Eph-NPs vaccine does not harm the liver or kidney.

Discussion

We created new biodegradable γ-PGA-Phe NPs for use as a new adjuvant [16]. Uto et al. [22] reported that γ-PGA-Phe NPs could activate DCs in vivo and cellular immunity

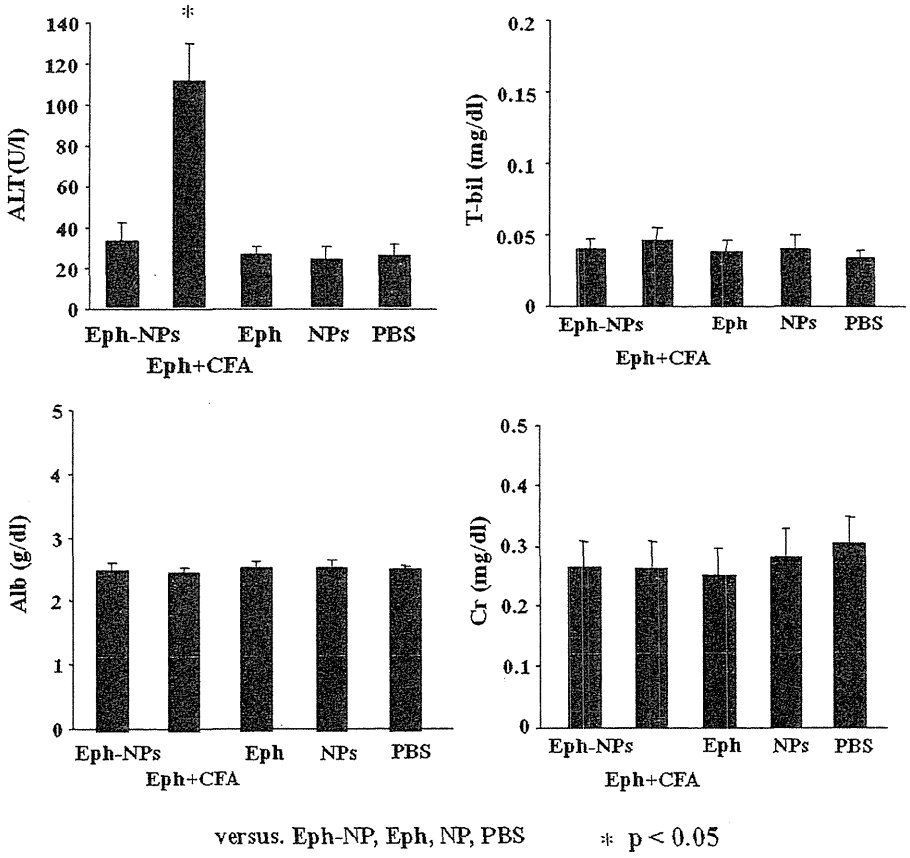

Fig. 5 Safety of Eph-NPs vaccine. Blood samples were obtained 7 days after final immunization of Eph-NPs, Eph + CFA, NPs, Eph or PBS. Levels of serum ALT, TBil, Alb or Crnn were examined. $N = 5$/group. $^*P < 0.05$ versus PBS group

against tumor cells expressing artificial antigen OVA. All previous reports using γ-PGA-Phe NPs as a vaccine adjuvant were evaluated with OVA artificial antigen models [22, 29–31]. Dhodapkar et al. [32] reported that the immunogenicity of peptides derived from self-melanoma antigens were very weak compared with viral protein-derived peptides. Although many TAA-derived peptides may be applicable to clinical use as peptide-based vaccines, most TAAs are self-antigens and not or weakly immunogenic, which is inferior to elicit enough anti-tumor immunity. Thus, the anti-tumor effect of γ-PGA-Phe NPs vaccines should be reevaluated by using self-TAA-derived peptides. In this study, we used EphA2-derived peptide [25] as a self-TAA. EphA2 is of particular interest due to evidence suggesting its involvement in carcinogenesis. EphA2 is a 130 kDa protein normally localized to sites of cell-to-cell contact, where it plays a role in contact growth inhibition [33]. However, cellular overexpression of EphA2, either as a result of its constitutive dysregulation or ectopic gene insertion, results in the disruption of cell-to-cell contacts, and enhancement of cell-to-extracellular matrix attachments [33]. As a result, tumor cells that overexpress EphA2 exhibit increased motility and invasive properties, consistent with a pro-metastatic phenotype [33]. Overexpression of EphA2 has been observed in numerous cancer types [34], including melanoma [35] and carcinomas of the breast [36, 37], lung [38], pancreas [39] and prostate [40]. We demonstrated the usefulness of Eph-NPs vaccine therapy, which revealed the future potential of clinical applications of this treatment in various cancers.

Complete Freund's adjuvant is an emulsion of water and mineral containing killed mycobacteria and has highly potent activity as an adjuvant. However, CFA administration induces adverse effects such as weight loss, neutrophilia and granulomatous peritonitis [41–43]. Consistent with earlier observations, immunization with Eph + CFA induced liver hepatocyte damage evidenced by elevation of ALT levels and granulomatous peritonitis in all of the mice. We demonstrated that immunization with Eph-NPs revealed anti-tumor effects against liver tumor via the generation of acquired immunity equal to the strongest but very toxic adjuvant, CFA, suggesting that our biodegradable γ-PGA-Phe NPs could be a promising candidate for a vaccine adjuvant against liver cancer.

IFN-γ ELISPOT assays revealed that immunization with Eph-NPs into normal mice resulted in induction of EphA2-derived peptide-specific CD8+ T cells at a level equivalent to Eph + CFA vaccine. Based on these results, we examined the anti-tumor effect of Eph-NPs vaccines in the EphA2-positive MC38 liver tumor model. The Eph-NPs vaccines resulted in eliciting anti-tumor effects against EphA2-positive MC38 liver tumor, but not against EphA2-negative BL6 melanoma, suggesting that EphA2-specific anti-tumor immunity was generated by Eph-NPs vaccines, which is consistent with our IFN-γ ELISPOT assay data. These results suggested that the anti-tumor potential of γ-PGA-Phe NPs vaccine is similar to that of CFA as an adjuvant in peptide-based vaccine. Importantly, Eph-NPs vaccine showed no toxic side effect on liver and kidney function. In contrast, CFA + Eph vaccine caused liver damage. γ-PGA-Phe NPs vaccine is safe and should be clinically applicable. This supports the clinical potential of γ-PGA-Phe NPs vaccine in cancer treatment.

In vitro cytotoxicity assays revealed that the anti-tumor effector cells for killing MC38 cells were CD8+ T cells, and possibly CTLs. This cytolytic activity was specific for MC38 cells because splenocytes did not kill BL6 cells. These results suggested that Eph-NPs vaccines could efficiently generate specific CTLs that recognize and kill relevant EphA2-positive, but not irrelevant EphA2-negative tumor targets. The liver uniquely contains an abundance of not only T cells, but also NK cells and NKT cells when compared with other organs [44, 45]. We have previously reported that not only CD8+ T cells, but also NK cells are required for optimal anti-tumor effects associated with EphA2-derived peptide pulsed DCs vaccines in liver tumors [26]. In this study, liver NK cells were not activated by Eph-NPs vaccination. Spleen NK cells were also not activated by Eph-NPs vaccine, and naïve spleen cells co-cultured with γ-PGA-Phe NPs or Eph-NPs could not display cytolytic activity against YAC-1 targets (S. Yamaguchi et al., unpublished data). These results suggested that the Eph-NPs vaccine could activate acquired immunity specifically. Our in vivo lymphocyte depletion studies demonstrated that CD8+ T cells, not CD4+ T cells and NK cells, tended to contribute to the inhibition of liver tumor growth in Eph-NPs vaccine, although we could not deny the possibility that humoral immune responses against EphA2 may also be generated by Eph-NPs vaccine. Previous reports demonstrated that biodegradable NPs were taken up by dedicated professional antigen-presenting cells, such as DCs, which resulted in their subsequent migration to lymph nodes, increased production of cytokines, and enhanced expression of costimulatory molecules followed by antigen-presentation to T cells [22, 29, 30]. Eph-NPs taken by DCs were directly presented to T cells and the generated Eph-specific CD8+ CTL could serve as effector cells against EphA2 expressing MC38 tumor.

In spite of recent progress and early success reported for adjuvant peptide vaccine trials in the prevention of liver cancer, there remains a great need to develop novel and effective treatment modalities. In this study, we demonstrated that immunization with Eph-NPs vaccines revealed anti-tumor effects against liver cancers via acquired immunity equivalent to the strongest CFA and that Eph-NPs vaccines did not lead liver or kidney damage. These results

suggest that γ-PGA-Phe NPs could be a promising candidate for a vaccine adjuvant against liver cancer. We are now preparing for the clinical application of γ-PGA-Phe NPs-peptide vaccine against liver cancer.

Acknowledgments This work was supported by a Grant-in-Aid from Core Research for Evolutional Science and Technology (CREST) from Japan Science and Technology Agency (JST).

References

1. Berzofsky JA, Ahlers JD, Belyakov IM (2001) Strategies for designing and optimizing new generation vaccines. Nat Rev Immunol 1:209–219
2. Schijns VE (2000) Immunological concepts of vaccine adjuvant activity. Curr Opin Immunol 12:456–463
3. Valmori D, Souleimanian NE, Tosello V et al (2007) Vaccination with NY-ESO-1 protein and CPG in Montanide induces integrated antibody/Th1 responses and CD8 T cells through cross-priming. Proc Natl Acad Sci USA 104:8947–8952
4. Wang F, Bade E, Kuniyoshi C et al (1999) Phase 1 trial of a MART-1 peptide vaccine with incomplete Freund's adjuvants for resected high-risk melanoma. Clin Cancer Res 5:2756–2765
5. Gilewski TA, Ragupathi G, Dickler M et al (2007) Immunization of high-risk breast cancer patients with clustered sTn-KLH conjugate plus the immunologic adjuvant QS-21. Clin Cancer Res 13:2977–2985
6. Bottomley A, Debruyne C, Ferip E et al (2008) Symptom and quality of life results of an international randomized phase 3 study of adjuvant vaccination with Bec2/BCG in responding patients with limited disease small-cell lung cancer. Eur J Cancer 44:2178–2184
7. Perales MA, Yuan J, Powel S et al (2008) Phase 1/2 study of GM-CSF DNA as an adjuvant for a multipeptide cancer vaccine in patients with advanced melanoma. Mol Ther 16:2022–2029
8. Mocellin S, Riccardo-Rossi C, Lise M et al (2004) Colorectal cancer vaccines: principles, results, and perspectives. Gastroenterology 27:1821–1837
9. Dinauer N, Balthasar S, Weber C et al (2005) Selective targeting of antibody-conjugated nanoparticles to leukemic cells and primary T-lymphocytes. Biomaterials 26:5898–5906
10. Khatri K, Goyal AK, Gupta N et al (2008) Plasmid DNA loaded chitosan nanoparticles for nasal mucosal immunization against hepatitis B. Int J Pharm 354:235–241
11. Almeida AJ, Souto E (2007) Solid lipid nanoparticles as a drug delivery system for peptides and proteins. Adv Drug Deliv Rev 59:478–490
12. Hayakawa T, Kawamura M, Okamoto M et al (1998) Concanavalin A-immobilized polystyrene nanospheres capture HIV-1 and gp120: potential approach towards prevention of viral transmission. J Med Virol 56:327–331
13. Kawamura M, Naito T, Ueno M et al (2002) Induction of mucosal IgA following intravaginal administration of inactivated HIV-1-capturing nanospheres in mice. J Med Virol 66:291–298
14. Akagi T, Kawamura M, Ueno M et al (2003) Mucosal immunization with inactivated HIV-1-capturing nanospheres induces a significant HIV-1-specific vaginal antibody response in mice. J Med Virol 69:163–172
15. Miyake A, Akagi T, Enose Y et al (2004) Induction of HIV-specific antibody response and protection against vaginal SHIV transmission by intranasal immunization with inactivated SHIV-capturing nanospheres in macaques. J Med Virol 73:368–377
16. Akagi T, Wang X, Uto T, Baba M, Akashi M (2007) Protein direct delivery to dendritic cells using nanoparticles based on amphiphilic poly(amino acid) derivatives. Biomaterials 28:3427–3436
17. Shih IL, Van YT (2001) The production of poly-(γ-glutamic acid) from microorganisms and its various applications. Bioresour Technol 79:207–225
18. Obst M, Steinbüchel A (2004) Microbial degradation of poly(amino acid)s. Biomacromolecules 5:1166–1176
19. Sung MH, Park C, Kim CJ, Poo H, Soda K, Ashiuchi M (2005) Natural and edible biopolymer poly-γ-glutamic acid: synthesis, production, and applications. Chem Rec 5:352–366
20. Akagi T, Higashi M, Kaneko T et al (2005) In vitro enzymatic degradation of nanoparticles prepared from hydrophobically-modified poly(γ-glutamic acid). Macromol Biosci 14:598–602
21. Akagi T, Kaneko T, Kida T, Akashi M (2006) Multifunctional conjugation of proteins on/into bio-nanoparticles prepared by amphiphilic poly(γ-glutamic acid). J Biomater Sci Polym Ed 17:875–892
22. Uto T, Wang X, Sato K et al (2007) Targeting of antigen to dendritic cells with poly(gamma-glutamic acid) nanoparticles induces antigen-specific humoral and cellular immunity. J Immunol 178:2979–2986
23. Olson RM, Perencevich NP, Malcolm AW et al (1980) Patterns of recurrence following curative resection of adenocarcinoma of the colon and rectum. Cancer 45:2969–2974
24. Malcolm AW, Perencevich NP, Olson RM et al (1981) Analysis of recurrence patterns following curative resection for carcinoma of the colon and rectum. Surg Gynecol Obstet 152:131–136
25. Yamaguchi S, Tatsumi T, Takehara T et al (2007) Immunotherapy of murine colon cancer using receptor tyrosine kinase EphA2-derived peptide-pulsed dendritic cell vaccines. Cancer 110:1469–1477
26. Yamaguchi S, Tatsumi T, Takehara T et al (2008) Dendritic cell-based vaccines suppress metastatic liver tumor via activation of local innate and acquired immunity. Cancer Immunol Immunother 57:1861–1869
27. Akagi T, Kaneko T, Kida T et al (2005) Preparation and characterization of biodegradable nanoparticles based on poly(γ-glutamic acid) with L-phenylalanine as a protein carrier. J Control Release 108:226–236
28. Tatsumi T, Gambotto A, Robbins PD et al (2002) Interleukin 18-gene transfer expands the repertoire of anti-tumor Th1-type immunity elicited by dendritic cell- based vaccines in association with enhanced therapeutic efficacy. Cancer Res 62:5853–5858
29. Yoshikawa T, Okada N, Oda A et al (2008) Development of amphiphilic γ-PGA-nanoparticle based tumor vaccine: potential of the nanoparticle cytosolic protein delivery carrier. Biochem Biophys Res Commun 366:408–413
30. Yoshikawa T, Okada N, Oda A et al (2008) Nanoparticles built by self-assembly of amphiphilic γ-PGA can deliver antigens to antigen-presenting cells with high efficiency: a new tumor-vaccine carrier for eliciting effector T cells. Vaccine 26:1303–1313
31. Uto T, Wang X, Akagi T et al (2009) Improvement of adaptive immunity by antigen-carrying biodegradable nanoparticles. Biochem Biophys Res Commun 379:600–604413
32. Dhodapkar MV, Young JW, Chapman PB et al (2006) Paucity of functional T-cell memory to melanoma antigens in healthy donors and melanoma patients. Clin Cancer Res 6:4831–4838
33. Zantek ND, Azimi M, Fedor-Chaiken M, Wang B, Brackenbury R, Kinch MS (1999) E-cadherin regulates the function of the EphA2 receptor tyrosine kinase. Cell Growth Differ 10:629–638
34. DeRisi J, Penland L, Brown PO et al (1996) Use of a cDNA microarray to analyse gene expression patterns in human cancer. Nat Genet 14:457–460

35. Easty DJ, Hill SP, Hsu MY et al (1999) Up-regulation of ephrin-A1 during melanoma progression. Int J Cancer 84:494–501
36. Lu M, Miller KD, Gokmen-Polar Y, Jeng MH, Kinch MS (2003) EphA2 overexpression decreases estrogen dependence and tamoxifen sensitivity. Cancer Res 63:3425–3429
37. Zelinski DP, Zantek ND, Stewart JC, Irizarry AR, Kinch MS (2001) EphA2 overexpression causes tumorigenesis of mammary epithelial cells. Cancer Res 61:2301–2306
38. Branan JM, Dong W, Prudkin L et al (2009) Expression of the receptor tyrosine kinase EphA2 is increased in smokers and predicts poor survival in non-small cell lung cancer. Clin Cancer Res 15:4423–4430
39. Duxbury MS, Ito H, Zinner MJ, Ashley SW, Whang EE (2004) EphA2: a determinant of malignant cellular behavior and a potential therapeutic target in pancreatic adenocarcinoma. Oncogene 23:1448–1456
40. D'Amico TA, Aloia TA, Moore MB et al (2001) Predicting the sites of metastases from lung cancer using molecular biologic markers. Ann Thorac Surg 72:1144–1148
41. Broderson JR (1989) A retrospective review of lesions associated with the use of Freund's adjuvant. Lab Anim Sci 39:400–405
42. Amyx HL (1987) Control of animal pain and distress in antibody production and infectious disease studies. J Am Vet Med Assoc 191:1287–1289
43. Toth LA, Dunlap AW, Olson GA et al (1989) An evaluation of distress following intraperitoneal immunization with Freund' adjuvant in mice. Lab Anim Sci 39:122–126
44. George AP, Catherine AP (2005) Liver immunobiology. Toxicol Pathol 33:52–62
45. Doherty DG, O'Farrelly C (2000) Innate and adaptive lymphoid cells in human liver. Immunol Rev 174:5–20

Sorafenib Inhibits the Shedding of Major Histocompatibility Complex Class I–Related Chain A on Hepatocellular Carcinoma Cells by Down-Regulating a Disintegrin and Metalloproteinase 9

Keisuke Kohga,* Tetsuo Takehara,* Tomohide Tatsumi,* Hisashi Ishida, Takuya Miyagi, Atsushi Hosui, and Norio Hayashi

The ectodomain of major histocompatibility complex class I–related chain A (MICA) is shed from tumor cells, and may be an important means of evading antitumor immunity. This study investigated the roles of a disintegrin and metalloproteinase 9 (ADAM9) in the shedding of MICA in human hepatocellular carcinoma (HCC). Small interfering RNA–mediated knockdown (KD) of ADAM9 resulted in up-regulation of membrane-bound MICA expression on the HepG2 and PLC/PRF/5 cellular surfaces and down-regulation of soluble MICA levels in their culture supernatant. ADAM9 was cleaved at a site between Gln347 and Val348 of MICA *in vitro*. We constructed a plasmid of the MICA gene with mutation or deletion of the ADAM9 cleavage site to examine the detailed mechanism of MICA shedding by ADAM9 protease. The results suggested that MICA might be cleaved at the intracellular ADAM9-recognized cleavage site and was further cleaved at the extracellular ADAM9-independent cleavage site in HCC cells, resulting in the production of soluble MICA. Immunohistochemical analysis revealed that ADAM9 was overexpressed in human HCC compared to normal liver tissues. The cytolytic activity of natural killer (NK) cells against ADAM9KD-HCC cells was higher than that against control cells, and the enhancement of this cytotoxicity depended on the MICA/B and NK group 2, member D pathway. Sorafenib treatment resulted in decreased expression of ADAM9, increased expression of membrane-bound MICA expression, and decreased levels of soluble MICA in HCC cells. Adding sorafenib enhanced the NK sensitivity of HCC cells via increased expression of membrane-bound MICA. *Conclusion:* ADAM9 is involved in MICA ectodomain shedding in HCC cells, and sorafenib can modulate ADAM9 expression. Sorafenib therapy may have a previously unrecognized effect on antitumor immunity in patients with HCC. (HEPATOLOGY 2010;51: 1264-1273.)

Hepatocellular carcinoma (HCC) is one of the leading causes of cancer death worldwide. Chronic liver disease caused by hepatitis virus infection and nonalcoholic steatohepatitis leads to a predisposition for HCC; liver cirrhosis, in particular, is considered to be a premalignant condition.[1,2] With regard to treatment, surgical resection or percutaneous techniques such as ethanol injection and radiofrequency ablation are

Abbreviations: Ab, antibody; ADAM, a disintegrin and metalloproteinase; ELISA, enzyme-linked immunosorbent assay; HCC, hepatocellular carcinoma; HLA, human leukocyte antigen; KD, knockdown; MHC, major histocompatibility complex; MICA, MHC class I–related chain A; mRNA, messenger RNA; NK, natural killer cell; PBS, phosphate-buffered saline; RT-PCR, reverse transcription polymerase chain reaction; siRNA, small interfering RNA.

From the Department of Gastroenterology and Hepatology, Osaka University Graduate School of Medicine, Osaka, Japan.

Received October 8, 2009; accepted November 13, 2009.

**These authors contributed equally to this work.*

This work was supported by a Grant-in-Aid from the Ministry of Education, Culture, Sports, Science and Technology of Japan and a Grant-in-Aid for Research on Hepatitis and Bovine Spongiform Encephalopathy from the Ministry of Health, Labour and Welfare of Japan.

Address reprint requests to: Norio Hayashi, M.D., Ph.D., Department of Gastroenterology and Hepatology, Osaka University Graduate School of Medicine, 2-2 Yamadaoka, Suita, Osaka 565-0871, Japan. E-mail: hayashin@gh.med.osaka-u.ac.jp; fax: 81-6-6879-3629.

Copyright © 2009 by the American Association for the Study of Liver Diseases.

Published online in Wiley InterScience (www.interscience.wiley.com).

DOI 10.1002/hep.23456

Potential conflict of interest: Nothing to report.

Additional Supporting Information may be found in the online version of this article.

considered to be choices for curable treatment of localized HCC, whereas transarterial chemoembolization (TACE) is a well-established technique for more advanced HCC.[3] The liver contains both a large compartment of innate immune cells (natural killer [NK] cells and NK T cells) and acquired immune cells (T cells),[4,5] but the activation of these immune cells after HCC treatment remains unclear. If such treatments can efficiently activate abundant immune cells in the liver, this could lead to the establishment of attractive new strategies for HCC treatment.

Major histocompatibility complex (MHC) class I–related chain A (MICA) is a ligand for NK group 2, member D (NKG2D) receptors expressed on a variety of immune cells.[6] In contrast to classical MHC class I molecules, MICA is rarely expressed on normal cells but frequently on tumor cells.[7–10] The engagement of MICA and NKG2D strongly activates NK cells, enhancing their cytolytic activity and cytokine production.[11] Thus, the MICA-NKG2D pathway is an important mechanism by which the host immune system recognizes and kills transformed cells.[12] In addition to those membrane-bound forms, MICA molecules are cleaved proteolytically from tumor cells and appear as soluble forms in sera of patients with malignancy, including HCC.[13–17] The release of soluble MICA/MHC class I–related chain B (MICB) from tumor cells is thought to antagonize NKG2D-mediated immunosurveillance. Recently, members of the metzincin superfamily, such as disintegrin and metalloproteinase (ADAM) proteins have been reported to play essential roles in the proteolytic release of the ectodomain of transmembranous proteins, including MICA, from the cell surface.[14,18] MICA shedding of 293T fibroblast cells and HeLa cervical cancer cells was found to be inhibited by silencing of the ADAM10 and ADAM17 proteases.[19] We also demonstrated that ADAM10, but not ADAM17, proteases are associated with MICA shedding in human HCC.[20] However, it remains to be determined whether other ADAM proteases can affect MICA shedding.

Sorafenib is a unique multitargeting kinase molecule that inhibits the receptor tyrosine kinases (vascular endothelial growth factor receptor 2 [VEGFR-2], VEGFR-3, Flt-3, platelet-derived growth factor receptor [PDGFR], and fibroblast growth factor receptor 1) as well as Raf serine-threonine kinase in signal transduction. A recent phase III study, the Sorafenib HCC Assessment Randomized Protocol (SHARP), revealed that the median overall survival of sorafenib-treated patients with HCC was significantly higher than that of patients who received the placebo.[21] To develop further uses for sorafenib in HCC treatment, its immunological impact in HCC treatment needs to be evaluated.

In this study, we investigated the association of ADAM9 proteases with MICA shedding in human HCC cells. Of importance is the discovery that ADAM9 knockdown (KD) experiments revealed the essential roles of ADAM9 protease in the shedding of MICA molecules. Sorafenib, a multikinase inhibitor that has been recently approved as a new anti-HCC molecular targeted chemotherapy, was effective in down-regulating soluble MICA and up-regulating membrane-bound MICA via inhibition of ADAM9 protease, resulting in enhancing the NK sensitivity of sorafenib-treated HCC cells. This study sheds light on previously unrecognized effects of sorafenib on modulating ADAM9 and MICA shedding, and thus suggests promise for its use in chemoimmunotherapy against human HCC.

Materials and Methods

HCC Cell Lines. Human HCC cell lines HepG2 and PLC/PRF/5 were purchased from the American Type Culture Collection (Manassas, VA) and were cultured with Dulbecco's modified Eagle medium (DMEM) supplemented with 10% fetal bovine serum (GIBCO/Life Technologies, Grand Island, NY) in a humidified incubator at 5% CO_2 and 37°C.

Reagents. Sorafenib was kindly provided by Bayer HealthCare Pharmaceuticals Inc. (Wayne, NJ). The compound was dissolved in 100% dimethyl sulfoxide (DMSO) to a final concentration of 100 mM. The dissolved solution was diluted with DMEM supplemented with 10% heat-inactivated fetal bovine serum (Sigma, St. Louis, MO) to 1-15 μmol/L. HCC cell viability was determined at 72 hours after addition of 1-15 μmol/L sorafenib or DMSO by WST-8 assay using cell count reagent sulforaphane (Nacalai Tesque, Kyoto, Japan) as previously described.[20]

RNA Silencing. The small interfering RNA (siRNA) method was used to knockdown ADAM9 as previously described.[20] At 24 hours after transfection, the cells were analyzed for specific depletion of the messenger RNA (mRNA) of ADAM9 by real-time reverse transcription polymerase chain reaction (RT-PCR) according to the manufacturer's instructions (Applied Biosystems, Foster City, CA). The following siRNAs were used: ADAM9, 5′-UGUCCAAACACAUUAAUCCCGCCUG-3′; scramble control, 5′-UGUCGCACAAACACUUAACUCCCUG-3′.

Enzyme-Linked Immunosorbent Assay. HCC cells were cultured with tumor necrosis factor-α protease inhibitor-I (TAPI-I, 50 μmol/L; Calbiochem, San Diego, CA) or sorafenib (1 μmol/mL) for 24 hours and the supernatants were harvested. The supernatants of cultured HCC cells were harvested at 24 hours after transfection

with siRNA. The levels of soluble MICA were determined by DuoSet MICA enzyme-linked immunosorbent assay (ELISA) kit (R&D Systems, Minneapolis, MN).

Flow Cytometry. For the detection of membrane-bound MICA, cells were incubated with anti-MICA antibody (Ab) (Santa Cruz Biotechnology, Santa Cruz, CA) and stained with phycoerythrin-goat anti-mouse immunoglobulin (Ig) (Beckman Coulter, Fullerton, CA) as a secondary reagent and then subjected to flow cytometric analysis using a FACScan flow cytometer (Becton Dickinson, San Jose, CA).

Real-Time RT-PCR. Total RNA was isolated using the RNeasy Mini Kit (Qiagen K.K., Tokyo, Japan), and was reverse transcribed using SuperScript III First-Strand Synthesis System (Invitrogen, Carlsbad, CA). The mRNA levels were evaluated using ABI-Prism 7900 Sequence Detection System (Applied Biosystems). Ready-to-use assays (Applied Biosystems) were used for the quantification of ADAM9 (Hs00177638_m1), and β-actin (Hs99999903_m1) mRNAs according to the manufacturer's instructions. β-Actin mRNA from each sample was quantified as an endogenous control of internal RNA.

Mass Spectrometry Analysis to Determine the Cleavage Site. Peptides of 20 amino acid residues partially overlapping each other, covering the α3 domain to the C-terminal end of MICA were synthesized by Sigma. Each peptide substrate (30 μM) was incubated with 50 nM of recombinant ADAM9 in a buffer containing 10 mM HEPES (pH 7.2) and 0.0015% Brij (Sigma). After digestion, the samples were passed over a C18 media ($ZipTip_{C18}$; Millipore, Billerica, MA), eluted with acetonitrile, and analyzed by matrix-assisted laser desorption/ionization–time of flight/mass spectrometry (MALDI-TOF/MS) to determine the masses of the products and thereby the cleavage site recognized by ADAM9.

Plasmid Construction of pMyc-MICA. An expression vector of MICA, pcDNA-MICA, was constructed by using specific complementary DNA (cDNA) from the human hepatoma-derived cell line, Huh-7, as described.[20] The Myc-tag coding sequence was inserted between the putative leader peptide and the α1 domain of the MICA cDNA using QuikChange Site-Directed Mutagenesis Kit (Stratagene, La Jolla, CA), referred to as pMyc-MICA. For construction of pcDNA-MICA-mut or pMyc-MICA-mut, Val348 and Leu349 were substituted for alanine. pcDNA-MICA-del or pMyc-MICA-del, which expresses MICA (or myc-tagged MICA) truncated at Val348, was generated by introducing a stop codon after Gln347. The stop codon was inserted after Pro298, the C-terminus of the putative α3 domain, to construct soluble MICA expression vectors, pcDNA-MICA-sol or pMyc-MICA-sol. Cells were transfected with the MICA expression vectors using Lipofectamine LTX reagent (Invitrogen). As a control, cells were cotransfected with pEGFP-C1 (Clontech, Mountain View, CA) to monitor the transfection efficiencies.

Immunoprecipitation. The lysates of cells or tissues were prepared as previously described.[20] Immunoprecipitation with anti-c-Myc beads was performed for 1 hour at 4°C. Immunocomplexes were eluted by c-Myc tagged peptide solution (MBL, Woburn, MA). The samples after immunoprecipitation were treated with 250 mU of N-glycosidase F (Roche, Mannheim, Germany) for 3 hours at 37°C.

Western Blotting. The total cellular protein was electrophoretically separated by sodium dodecyl sulfate-12% polyacrylamide gels and transferred onto polyvinylidene fluoride membrane. The membrane was blocked in Tris-buffered saline-Tween containing 5% skim milk for 1 hour, and then probed with anti-Myc mouse monoclonal antibody (mAb) (Cell Signaling Technology, Danvers, MA), anti-ADAM9 mAb (R&D Systems) at 4°C overnight. Horseradish peroxidase–conjugated anti-rabbit Ab and SuperSignal West Pico System (Pierce, Rockford, IL) were used for the detection of blots.

Liver Tissues and Immunohistochemistry. Human HCC tissues (n = 11) obtained at surgical resection were used. Informed consent, under a protocol approved by Institutional Review Board, was obtained from all patients before sample acquisition. Liver sections were subjected to immunohistochemical staining using the ABC procedure (Vector Laboratories, Burlingame, CA). The primary Ab used was anti-ADAM9 (R&D Systems). To confirm the specificity of the staining, primary antibodies were incubated with recombinant ADAM9 protein (R&D Systems) for 3 hours and then applied onto liver sections in parallel with staining of the primary Abs as the absorption test.

NK Cell Analysis. NK cells were isolated from human peripheral blood mononuclear cells by magnetic cell sorting using CD56 MicroBeads according to the manufacturer's instructions (Miltenyi Biotec, Auburn, CA). The cytolytic abilities of NK cells against ADAM9KD/control HCC cells or 0.5 or 1 μmol/L sorafenib-treated HCC cells were assessed by 4-hour ^{51}Cr-releasing assay with or without MICA/B-blocking Ab (6D4; a generous gift from Dr. Veronika Groh and Dr. Thomas Spies, of the Fred Hutchinson Cancer Research Center, Seattle, WA),[7] which binds to the α1 and α2 domains of MICA.

Statistics. All values were expressed as the mean and standard deviation. The statistical significance of differences between the groups was determined by applying the Student *t* test or two-sample *t* test with Welch correction after each group had been tested with equal variance and

Fisher's exact probability test. We defined statistical significance as $P < 0.05$.

Results

TAPI-I Blocked the Shedding of MICA in Human HCC. We added TAPI-I, an α-secretase inhibitor, to human HCC cells and evaluated the membrane-bound MICA and soluble MICA production in human HCC. Both HepG2 cells and PLC/PRF/5 cells expressed membrane-bound MICA and produced soluble MICA in the culture supernatants (Fig. 1A). Membrane-bound MICA expression increased and the production of soluble MICA decreased after TAPI-I treatment in both HepG2 and PLC/PRF/5 cells. These results suggested that the modification of MICA expression on HCC cells might depend on an α-secretase, such as ADAM9, ADAM10, ADAM12, and ADAM17. We had previously investigated the roles of ADAM10 and ADAM17 in the shedding of MICA in human HCC[20] and found that ADAM12 was not expressed in human HCC cells (data not shown). In this study, we further investigated the involvement of ADAM9.

ADAM9 Was Involved in MICA Shedding of HCC Cells. To examine the involvement of ADAM9 in MICA ectodomain shedding, ADAM9 was knocked down in HCC cells using a siRNA-mediated procedure (ADAM9KD). The expression of ADAM9 was clearly suppressed in HepG2 cells and PLC/PRF/5 cells at mRNA levels (Fig. 1B). KD of ADAM9 for both types of HCC cells resulted in increasing membrane-bound MICA and decreasing soluble MICA levels in their culture supernatant (Fig. 1C). These results suggested that ADAM9 is critically involved in the shedding of MICA in HCC cells.

***Identification of the ADAM9 Cleavage Site of MICA* In Vitro.** Because ADAM9 KD clearly suppressed MICA shedding, we next tried to examine whether ADAM9 is capable of cleaving MICA directly. For this purpose, we carried out an in vitro cleavage assay using recombinant ADAM9 and several synthetic polypeptides which carried the MICA amino acid sequences. After the reaction, the polypeptides were subjected to MALDI-TOF/MS analysis. One of the polypeptides, KTSAAEGPELVSLQVLDQHP, was found to be cleaved by ADAM9. According to the calculated masses, the polypeptide was cleaved between Gln347 and Val348 (Fig. 2A). Based on these data, we constructed a plasmid of Myc-tagged MICA gene with mutation at the ADAM9 cleavage site ("VL" to "AA", pMyc-MICA-mut; Fig. 2A,B), a plasmid of Myc-tagged MICA gene with a stop codon at Val348 (pMyc-MICA-del, the truncated type of MICA gene; Fig. 2B) and a plasmid of Myc-tagged soluble MICA (pMyc-MICA-sol; Fig. 2B).

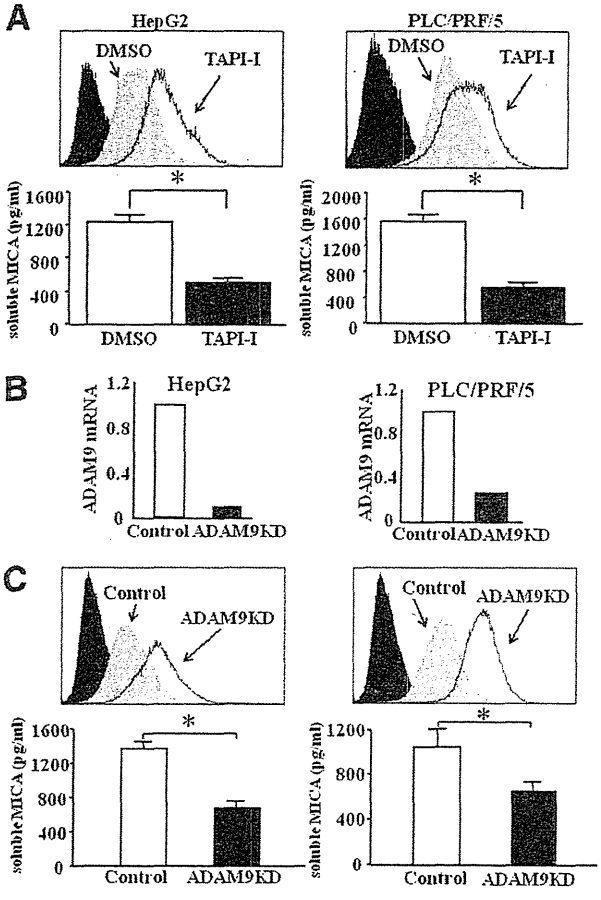

Fig. 1. ADAM9 was involved in the shedding of MICA in human HCC. (A) We added TAPI-I (50 μmol/L) to HepG2 or PLC/PRF/5 cells for 24 hours and evaluated the membrane-bound MICA on HCC cells by flow cytometry and soluble MICA production from HCC cells by ELISA. Black histogram, control IgG staining; gray histogram, anti-MICA staining of control HCC cells. Black line, anti-MICA staining of TAPI-I-treated HCC cells; white or black bar, soluble MICA from control HCC cells or TAPI-I-treated HCC cells, respectively. Representative results are shown. Similar results were obtained from three independent experiments. *$P <$ 0.05. (B) HCC cells (HepG2 and PLC/PRF/5) were treated with ADAM9 siRNA or control siRNA, and subjected to analysis of ADAM9 expressions by real-time RT-PCR. (C) The expressions of membrane-bound MICA on HCC cells treated with ADAM9 siRNA (ADAM9KD, black line) or control siRNA (Control, dotted line) were evaluated by flow cytometry. Closed histograms indicate control IgG staining. Soluble MICA production from HCC cells treated with ADAM9 siRNA or control siRNA were evaluated by specific ELISA. *$P < 0.05$. Representative results are shown. Similar results were obtained from three independent experiments.

Cell-lysates of pMyc-MICA or pcDNA-Myc, a control vector, transfected cells were collected and deglycosylated with tunicamycin. *In vitro* cleavage assay revealed that the size of full-length MICA was 43 kD, whereas the size of the MICA molecule cleaved by ADAM9 was 39 kD (Fig. 2C, lane 1 and 2), indicating

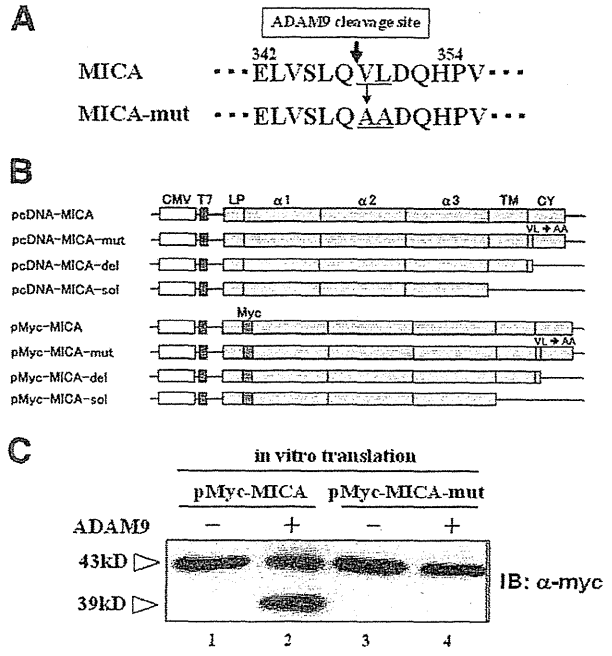

Fig. 2. MICA can be a substrate of ADAM9 according to an *in vitro* cleavage assay. (A) Synthetic polypeptides of MICA were incubated with recombinant ADAM9 and analyzed by MALDI-TOF/MS to identify the cleavage site. One of the synthetic polypeptides, KTSAAEGPELVSLQV-LDQHP, was found to be cleaved between Gln347 and Val348. Underlined amino acids Val348 and Leu349 were substituted with alanine as shown in (B) to construct mutant MICA (MICA-mut). (B) Scheme depicting MICA and Myc-tagged MICA expression vectors. CY: cytosolic domain; LP, leader peptide; TM, transmembrane domain. For details, see Materials and Methods. (C) Cleavage of MICA and mutant MICA by recombinant ADAM9. *In vitro*-translated Myc-MICA and Myc-MICA-mut were incubated with recombinant ADAM9 or left untreated, then analyzed by immunoblot using anti-myc-tag mAb.

that full-length MICA was an ADAM9 substrate as well as the polypeptide with a partial MICA sequence. To examine whether ADAM9 could directly cleave the identified ADAM9 cleavage site of MICA, *in vitro*–translated products of pMyc-MICA and pMyc-MICA-mut were treated with ADAM9, followed by immunoblot analysis. The 39-kD product of MICA cleaved by ADAM9 was not detected in the cleavage reaction using pMyc-MICA-mut (Fig. 2C, lane 3 and 4). These results suggested that ADAM9 directly cleaved MICA at the identified ADAM9 cleavage site *in vitro*.

Ectodomain Shedding of MICA Required a Step of Cytosolic Domain Truncation Mediated by ADAM9. To examine whether ADAM9 cleavage site was associated with the ectodomain shedding of MICA in HCC cells, we transfected a vector of the MICA gene (pcDNA-MICA), a vector of the MICA gene with mutation at the ADAM9 cleavage site (pcDNA-MICA-mut) or a control vector (pcDNA3) into HepG2 cells and collected the culture supernatants. Soluble MICA levels from pcDNA-MICA transfectants were significantly higher than those from pcDNA3 transfectants. In contrast, transfection of pcDNA-MICA-mut yielded similar levels of soluble MICA as seen with pcDNA3 control transfection (Fig. 3A). Transfection efficacies were similar among all transfectants, as indicated by green fluorescent protein (GFP)-positive rates (Fig. 3A).

We next transfected expression vectors of Myc-tagged MICA gene (pMyc-MICA), Myc-tagged MICA gene with mutation at ADAM9 cleavage site (pMyc-MICA-mut), or a control vector (pcDNA-Myc) into HepG2 cells and collected the culture supernatants. Immunoprecipitates from those samples with anti-Myc antibody were subjected to western blot analysis after deglycosylation with N-glycanase. Soluble MICA was detected in the supernatants of pMyc-MICA–transfected cells, but not in either pMyc-MICA-mut or pcDNA-Myc–transfected cells (Fig. 3B, upper panel). To verify whether the myc-tagged MICA molecules expressed in the cells were actually transported to the cell surface, we evaluated Myc-tag–positive cells by flow cytometry. Myc-tag–positive rates of pMyc-MICA and pMyc-MICA-mut transfectants were significantly higher than those of pcDNA-Myc transfectants, whereas those of pMyc-MICA transfectants were similar to those of pMyc-MICA-mut transfectants (Fig. 3B). Suemizu et al. have also demonstrated that the "VL" to "AA" mutation did not influence the polarization of MICA expression to the cell surface, which is consistent with our results.[22] Taken together, although mutation at the ADAM9 cleavage site did not alter the efficiency of the plasma membrane translocation of MICA, it dramatically inhibited the shedding of MICA, suggesting that the ADAM9 cleavage site has a critical role in the development of soluble MICA. To examine the molecular weight of MICA present in the cells, we transfected pMyc-MICA into control HepG2 or ADAM9KD-HepG2 cells. The whole-cell lysates were immunoprecipitated by anti-Myc Ab and then treated with N-glycanase. In control HepG2 cells, in addition to full-length MICA, two bands with molecular weights of 39 kD and 37 kD were detected (Fig. 3C), whereas neither of them was detected in ADAM9KD-HepG2 cells. These results suggested that ADAM9 protease was required for production of both the 39-kD product and the 37-kD product of MICA in HCC cells. The *in vitro* translation experiment revealed that the 39-kD product corresponded to ADAM9-cleaved MICA at the aforementioned ADAM9 cleavage site and the 37-kD product corresponded to final soluble MICA proteins formed by the second cleavage of the 39-kD, ADAM9 cleaved product. With respect to these data, two possibilities were